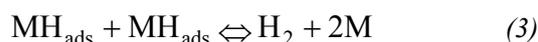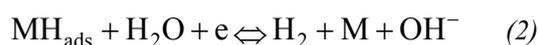*VLADIMIR D. JOVIĆ*

Composite materials based on non-noble metals as the cathodes in industrial electrolysis

Almost all cathodes in the industrial processes of hydrogen evolution, particularly for chlor-alkali electrolysis, are based on coatings containing noble metals (Pt,Ru,Ir etc.). Based on the theory of electrocatalysis of hydrogen evolution reaction (HER), in this work an attempt was made to produce Ni based cathode coatings containing MoO_3 or MoO_2 particles and investigate their behavior as cathodes for HER in concentrated NaOH solution. It is shown that it is possible to obtain coatings possessing the same overvoltage for HER as the one for commercial cathodes under the conditions of industrial electrolysis. In order to find optimal conditions for their electrodeposition all coatings were investigated by SEM, EDS and XRD analysis.

1. INTRODUCTION

The HER is one of the reactions most frequently occurring in industrial cells, either as wanted (electrolysis of water) or by-product reaction (chlor-alkali process) [1]. It is generally accepted, that the mechanism of the HER in aqueous alkaline solutions involves three basic steps, two electrochemical and one chemical, such as: the proton discharge electrosorption (Volmer reaction, Eq. (1)), electro-chemical desorption. (Heyrovsky reaction Eq. (2)) and H recombination (Tafel reaction Eq. (3)).

$$M + H_2O + e \Leftrightarrow MH_{ads} + OH^- \qquad (1)$$

$$MH_{ads} + H_2O + e \Leftrightarrow H_2 + M + OH^- \qquad (2)$$

$$MH_{ads} + MH_{ads} \Leftrightarrow H_2 + 2M \qquad (3)$$

It proceeds through limited number of steps with only one type of intermediate and this is the reason why only for this reaction complete theory of elec-trocatalysis has been developed [2]. According to the theory electrocatalytic activity depends on the heat of adsorption of the intermediate (H_{ads}) on the electrode surface, defined by well-known "volcano" curve pre-sented in Fig. 1 [1]. Although the most active metals for HER are noble metals placed on top of the "vol-cano" curve, it has been suggested that a combination of two metals from the two branches of "volcano" curve could results in enhanced activity for HER [3].

Address author: Institute for Multidisciplinary Research, Kneza Višeslava 1, 11030 Belgrade, Serbia
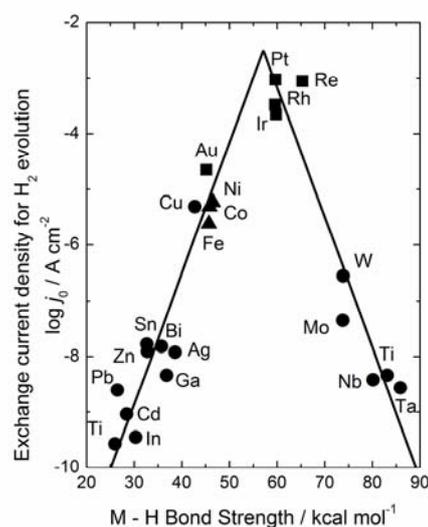
Figure 1. "Volcano" curve.

For industrial application it is important to reduce the overvoltage for the HER by electro-catalysis. This could be achieved by the increase of the real surface area (geometric factors) and by the change of the Tafel slope (electronic factors) [1]. If the Tafel slope changes, this is clear indication for the true catalytic effect.

During the past thirty years the most investigated were Mo-based alloys since they showed superior properties for HER. The investigation of the kinetics and the mechanism of the HER at the electrodepo-sited Ni-Mo alloys of various compositions has been the subject of numerous studies [4-14]. In some studies it was shown that the activity enhancement was mainly due to increased surface area [8,13], while there was also an evidence for clear synergetic effects (Tafel slope of 40 mV dec^{-1} extended to very high current densities [15]).

In this work an attempt was made to electro-deposit composite Ni-MoO$_x$ and Ni-MoO$_2$ coatings and investigate their catalytic effect for HER in connection with their composition and surface roughness.

2. EXPERIMENTAL

2.1. The cell and deposition conditions

The Ni-MoO$_x$ samples were deposited from the Watt's type electrolyte containing MoO$_3$ powder particles in the apparatus presented in Fig. 2. The volume of the electrolyte in the cell for deposition was approximately 20 dm^3. The electrolyte was circulated with the pump of a constant flow rate of 0.83 dm^3 s^{-1} (Fig. 1a). The flow rate in the cell was measured with a flow meter (Fig. 2a), being 0.33 dm^3 s^{-1}. Additional mixing of the electrolyte was provided by the air flow of 0.83 dm^3 s^{-1} through two pipes with small openings facing the bottom of the cell in order to remove eventually precipitated molybdenum oxide particles from the bottom of the cell and force particles to float and circulate with the electrolyte (schematically presented in Fig. 2b). The temperature of the electrolyte was kept constant by the thermocouple, heater and the control unit (Fig. 2a). The Ni mesh cathode, connected to a Ni holder (frame), was placed between two Ni anode plates (all of them of the dimensions 18 x 22 cm), as is schematically presented in Fig. 2b. A home made power supply, with the ripple smaller than 1 %, was used for applying necessary current/voltage. The Watt's type electrolyte was prepared from analytical grade chemicals dissolved in de-ionized water and the pH was adjusted at 4.5 by adding sulfuric acid. The samples of Ni-MoO$_x$ were deposited at the temperature of 50 °C and j = -25 mA cm^{-2} or j = -38 mA cm^{-2}. Before the deposition of Ni-MoO$_x$ coatings, the Ni meshes were etched in 2:1 HNO$_3$:H$_2$O solution for 60 s.
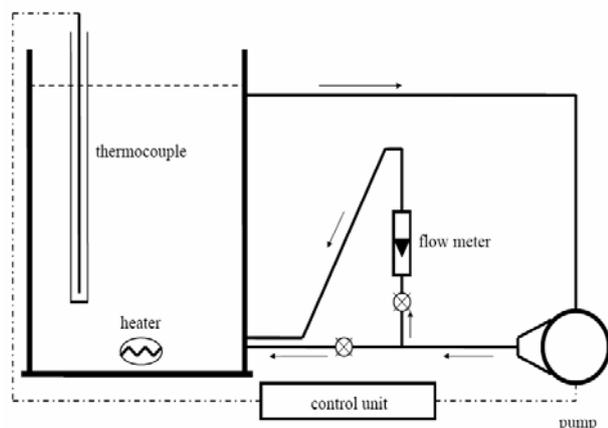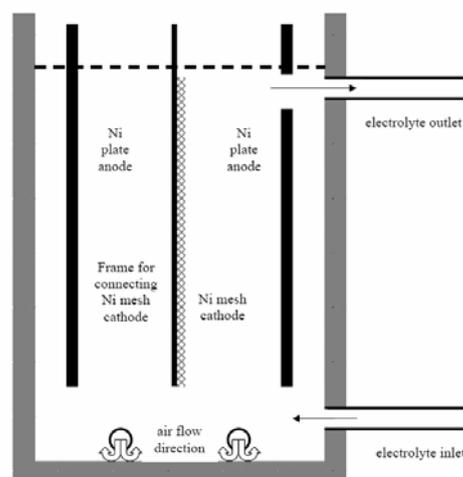

Fig. 2a

Fig 2b

Figure 2. Schematic presentation of the apparatus (a) and the cell (b) for electrochemical deposition of coatings.

2.2. Preparation of molybdenum oxide powders

The MoO$_3$ powder was prepared by thermal decomposition of (NH$_4$)$_6$Mo$_7$O$_{24}$·4H$_2$O at the temperature of 500 °C for 2 hours in the air atmosphere. The average particle size is estimated to be about 650 nm, according to the Sherrer formula from x-ray data. The MoO$_2$ powder was synthesized by rheological phase reaction route [16]. All reagents were analytical grade and used without further purification. Ammonium heptamolybdate (NH$_4$)$_6$Mo$_7$O$_{24}$·4H$_2$O and oxalic acid, C$_2$H$_4$O$_2$·2H$_2$O were fully mixed by grinding in ball mil with a molar ratio 1 : 1.05. A proper amount of absolute alcohol was added to get a rheological body. The mixture was sealed in a closed container at 80 °C for 8 hours. After drying in an oven at 80 °C, the white precursor was obtained. The XRD pattern of the product obtained at 400 °C was ascribed to a pure MoO$_2$ phase with the average particle size of about 850 nm, according to the Sherrer formula.

2.3. Polarization characteristics of Ni-MoO$_x$ and Ni-MoO$_2$ samples

The polarization characteristics of samples were tested in 32 wt.% NaOH solution at 90 °C. Experiments were performed in a standard electrochemical cell with Pt counter electrode and saturated calomel electrode (SCE) as the reference electrode. Electrodes were first submitted to hydrogen evolution at a constant current density of -0.1 A cm^{-2} for 1 h and after such pre-electrolysis polarization curves correcetd for IR drop were recorded using potentiostat Reference 600 and PHE 200 Software, (Gamry Instruments Inc.).

2.4. SEM, EDS and XRD analysis of the mesh surfaces and their cross section

The appearance and the composition of coated mesh surfaces and the cross sections of the coatings were investigated by SEM, Tescan, VEGA TS 5130 MM equipped with an energy-dispersive X-ray spectroscopy (EDS), INCAP enta FET-x3, Oxford Instruments. X-ray analysis was performed with X'PertPRO, PANalytical.

3. RESULTS AND DISCUSSION

3.1. Characterization of Ni-MoO$_x$ coatings

In Fig. 3 are compared polarization characteristics of commercial electrode (DN) and the best electrodeposited sample, el-1 (in the inset are shown j-t responses recorded at each applied potential – marked in the figure for the DN sample). It appears that these two electrodes are almost identically active for hydrogen evolution, with el-1 being slightly better at lower current densities ($j < 40$ mA cm^{-2}) and DN being better at higher current densities.
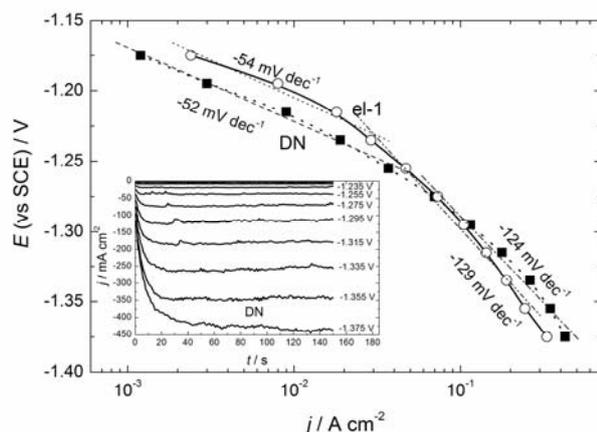

Figure 3. Polarization curves for HER onto commercial DN and Ni-MoO$_x$ electrode (el-1). Inset: j-t responses recorded at potentials used for determination of the polarization curve.

At the current density of 0.3 A cm^{-2} (usually used in industrial processes) the overvoltage for hydrogen evolution for the el-1 is for about 16 mV higher than that for DN electrode. It is well known that in a whole potential range for HER on the Ni electrode only one Tafel slope of about –120 mV dec^{-1} is present [17]. At the same poten-tial, the activity of Ni-MoO$_x$, as well as DN, is for about four orders of magnitude higher than that of Ni electrode. It is clear from the morphological investi-gations that the introduction of MoO$_3$ particles into Ni deposit produce rougher coatings (see Fig. 4), but undoubtedly syner-getic

effects are achieved, because the Tafel slopes decrease to – 54 mV dec^{-1} in the lower potential region and extends to relatively high current densities (about -20 mA cm^{-2}). It has been recently shown that the reaction mechanism of the HER on Ni is a consecutive combination of Volmer and Heyrovsky step [18] and that Heyrovsky step prevails over Tafel step in low overpotential region and the reaction rate is controlled by the Heyrovsky reaction with the almost full coverage by H$_{ads}$. However, the presence of Tafel slope of – 54 mV dec^{-1} for HER on Ni-MoO$_x$ indicates that Heyrovsky step controls the rate of the overall reaction in lower potential range, but with low coverage by H$_{ads}$ intermediates. In accordance with the mechanism of the HER, both Volmer and Heyrovsky steps occur at a single adsorption site and reaction takes place at Ni with almost full coverage by H$_{ads}$, while in the case of Ni-MoO$_x$ with low coverage by H$_{ads}$. The fact that the reaction rate is almost four orders of magnitude higher on the Ni-MoO$_x$ and commercial electrode indicates an increased catalytic activity of adsorption sites for the HER on both the electrodes in comparison with Ni.

3.1.1. SEM, EDS and XRD analysis of the el-1 sample

SEM micrograph of the surface of el-1 sample is shown in Fig. 4a, while its cross-section analysis is presented in Fig. 4b. As can be seen el-1 sample possesses cracks on the surface (Fig. 4a) going down to the substrate surface (Fig. 4b) with the thickness of the coating being about 25 μm. The results of the EDS of a cross section showed that the composition of the coating from the surface to the substrate is practically uniform: spectra 2 and 3 were of the same composition (76 at.% O, 8 at.% Ni, 22 at.% Mo). From the presented results it is obvious that at 2 g dm^{-3} of MoO$_3$ in this bath, under applied hydrodynamic conditions, sufficiently high amount of MoO$_x$ was incorporated in the deposit, making the coating catalytic for hydrogen evolution (almost the same as commercial electrode). According to the literature, solubility of MoO$_3$ is very small in cold water (1.066 g dm^{-3} at 18 ^{o}C) increasing with the temperature to 20.55 g dm^{-3} at 70 ^{o}C [19]. Obviously, in 20 dm^{-3} of the electrolyte at 50 ^{o}C significant amount of MoO$_3$ is dissolved (forming molybdic acid; H$_2$MoO$_4$·H$_2$O or MoO$_3$·2H$_2$O) and with this amount of MoO$_3$, under given hydrodynamic conditions, induced co-deposition of both metals occurs (the source of molybdenum being molybdate anion) producing deposits with observed morphology (presence of cracks) and composition. It is quite possible that such coating will not be stable in 32 wt. % NaOH at 90 ^{o}C for a long time operation, particularly during the shut down of the electrolysis.

SEM MAG: 80 x   DET: SE Detector
HV: 20.0 kV   DATE: 06/29/09   500 um   Vega ©Tescan
VAC: HiVac   Device: VEGA TS 5130MM   Digital Microscopy Imaging   *a)*
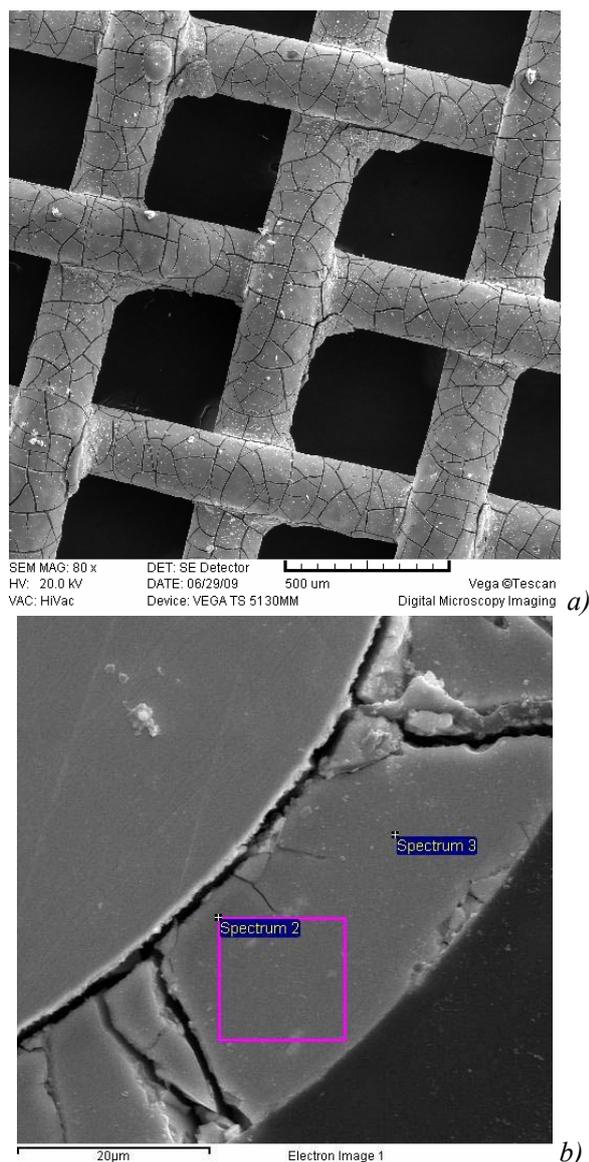

20μm   Electron Image 1   *b)*

*Figure 4. (a) SEM analysis of the el-1 sample surface.
(b) EDS analysis of the cross-section of el-1.*

In order to define eventual phases present in above mentioned coatings as-deposited sample of the el-1 was analysed by the XRD. Fig. 5a shows that only peaks for Ni could be detected on such sample. Taking into account recent results on the analysis of recrystallized Ni-Mo-O powders [20] one could expect that after annealing such sample at 300 ^oC for 5 h in air crystallites of other present phases would increase and become visible on the diffractograms. This has exactly happened during the annealing, as shown in the same figure (300 ^oC). Among the peaks of Ni (Ni) well defined peaks of MoO_3 (↑) and MoO_2 (↕) were detected on the diffractogram confirming that these two phases were deposited together with Ni in the Ni-MoO_x coatings. After additional annealing of the same sample at 600 ^oC for 5 h a new phase, $NiMoO_4$ (↓) has been detected, the peaks for MoO_3

(↑) phase disappeared, while some peaks of the MoO_2 (↕) phase remained on the diffractogram. At the same time weak reflections of NiO phase (▼) could be detected on this diffractogram (600 ^oC). Such behaviour is clear evidence that the $NiMoO_4$ phase has been formed by the solid state reaction between MoO_3 and NiO [20,21] during the annealing procedure at 600 ^oC. The presence of MoO_3 (↑) phase could be the results of two processes: MoO_3 particles were embedded in the deposit, or this phase is a product of induced co-deposition mechanism recently presented in the literature [21]. Taking into account the appearance of the deposit, particularly its cross section, it seems that a small amount of MoO_3 particles has been embedded in the deposit being reduced to MoO_2 particles (Fig. 7), while most of the MoO_3 phase was the results of induced co-deposition mechanism [21]. In the case of Watt's type electrolyte, assuming that MoO_3 has been dissolved forming $H_2MoO_4 \cdot H_2O$, the deposition of MoO_3 phase (in accordance with the previously suggested mechanism [21]) could be described by the following reaction:
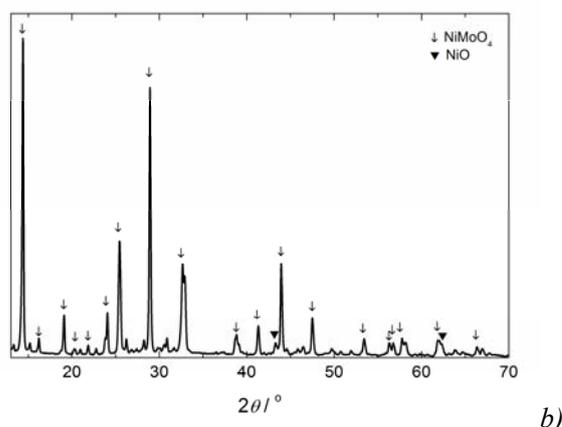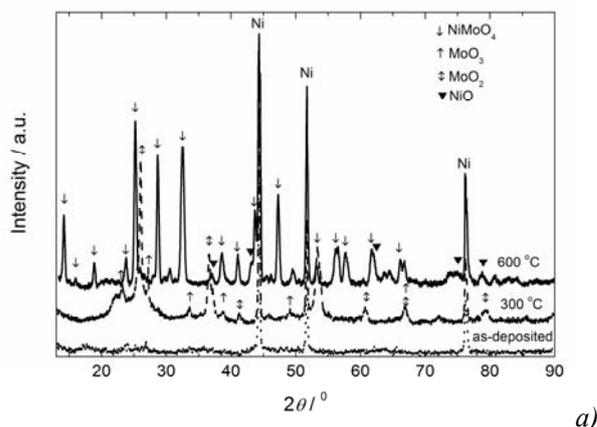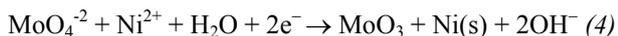

a)

b)

Figure 5. (a) XRD of as-deposited el-1 sample and the same sample after annealing at 300 ^oC and 600 ^oC for 5 h. (b) XRD of the part of coating that has been pilled off after annealing at 600 ^oC.

$$MoO_4^{-2} + Ni^{2+} + H_2O + 2e^- \rightarrow MoO_3 + Ni(s) + 2OH^- \quad (4)$$

Certain amount of the deposit has been pilled off from the Ni mesh during the annealing procedure and this powder was also analysed by XRD. Corresponding diffractogram is presented in Fig. 5b. As can be seen this part of the deposit contains mainly NiMoO₄ phase with a small amount of NiO phase, with no presence of Ni peaks (which mainly correspond to the mesh substrate on other diffractograms), indicating that this phase is brittle and cannot remain as a whole in the deposit on the Ni mesh after annealing at 600 °C. It is interesting to note that the presence of MoNi₄ phase has not been detected in the deposit, although it should exist according to the TEM analysis presented recently [21]. There are two reasons for the absence of the MoNi₄ phase in the deposit after annealing procedure: (*i*) taking into account that in the as-deposited Mo-Ni-O powders this phase is more strongly bound to the amorphous phase than MoO₃ phase [21], it is most likely that this particular phase is composed of nanocrystals which cannot be detected by the XRD even after annealing at 600 °C for 5 h; (*ii*) the induced co-deposition mechanism for deposition of MoNi₄ phase is defined by the formation of adsorbed species (either $[NiCitMoO_2]_{ads}^-$ or $[Ni(NH_3)_3MoO_2]_{ads}^{2+}$ - depending on the electrolyte composition) which further reduce to metallic Mo [21]. Taking into account that in the investigated Watt's type electrolyte neither $NiCit^-$ nor $[Ni(NH_3)_3]^{2+}$ complexes exist (nickel is present as Ni^{2+} ion) the formation of adsorbed species is not possible and, accordingly, molybdenum cannot be reduced into metallic state to produce MoNi₄ phase.

3.2. Characterization of Ni-MoO₂ coatings

In contrast to MoO₃, molybdenum dioxide, MoO₂ is practically insoluble in alkaline solutions, HCl, HF, and is only slightly soluble in hot H₂SO₄ [19]. According to the literature data [22,23] a suitable bath, which can operate at high current densities for Ni deposition, appeared to be bath composed of 0.2 M NiCl₂ and 2.0 M NH₄Cl. Regarding the unique features of MoO₂, such as metallic conductivity and chemical stability, an attempt was made to deposit Ni-MoO₂ coatings from this electrolyte containing suspended MoO₂ powder particles at room temperature in the cell and with the apparatus presented in Fig. 1.

Four samples were deposited at j = -300 mA cm⁻². Samples 1 and 2 were deposited from the bath with freshly added MoO₂ (1 and 2 g dm⁻³ respectively, after 1 h of electrolyte circulation), while deposition of samples 3 and 4 (2 and 3 g dm⁻³ respectively) started 24 h after MoO₂ addition. It appeared that

aging of the electrolyte of at least 24 h is necessary for better incorporation of MoO₂ particles in the deposit. Polarization characteristics for samples 1-4 are presented in Fig. 6a. A significant decrease of overvoltage for hydrogen evolution is recorded for samples 3 and 4. By comparing polarization curves of DN and the best sample 4 one can see that these two polarization curves are practically identical, Fig. 6b.
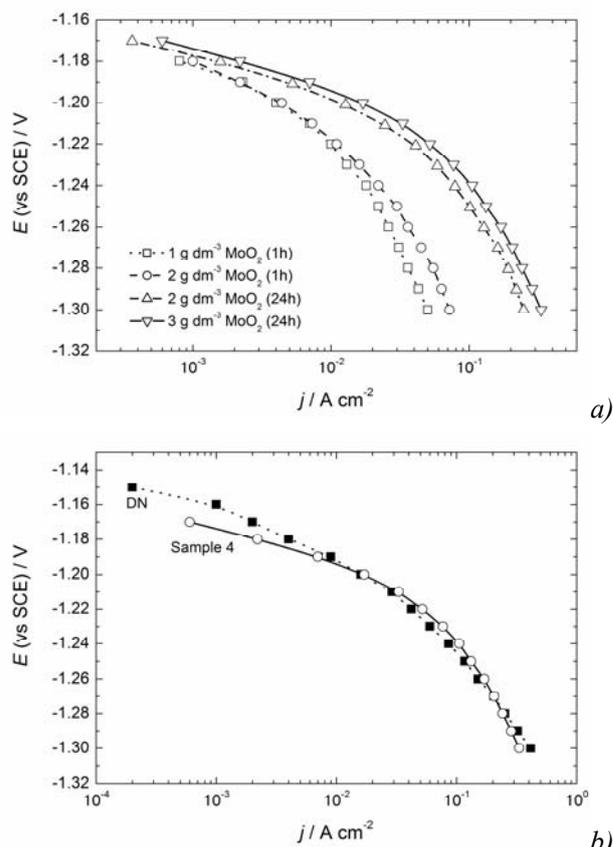

Figure 6. (a) Polarization curves for samples 1-4. (b) Polarization curves for DN and sample 4.
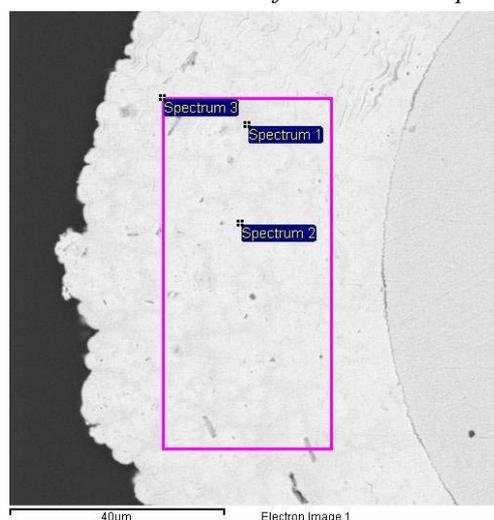

Figure 7. SEM and EDS analysis of a cross-section of sample 4.

Most of the coating of samples 3 and 4 is composed of homogeneously distributed Ni rich (grey) and Mo rich (white) areas, as shown on the back scatter SEM in Fig. 7. Such morphology is much more promising for a long time operation of the Ni-MoO$_2$ cathode.

4. CONCLUSIONS

From the presented results it could be concluded that the best catalytic activity for hydrogen evolution, with the polarization characteristic being identical to that of the commercial DN electrode, could be obtained for either Ni-MoO$_x$ or Ni-MoO$_2$ composite coatings, with the morphology of Ni-MoO$_2$ cathode being much more promising for a long time operation.

REFERENCES

[1] S. Trassatti, Advances in electrochemical science and engineering, Eds. H. Gerischer and C.W. Tobias, Vol. 2, Ch. 1, VCH, Germany, 1992, pp. 1-86.

[2] R. Parsons, Trans. Faraday Soc. 1958, 54, 1053-1063.

[3] M.M. Jakšić, Electrchim. Acta 1984, 29, 1539-1550.

[4] B.E. Conway, L. Bai, M.A. Sattar, Int. J. Hydrogen Energy 1987, 12, 607-621.

[5] I.A. Raj, K.I. Vasu, J. Appl. Electrochem. 1992, 22, 471-477.

[6] B.E. Conway, L. Bai, D.F. Tessier, J. Electroanal. Chem. 1984, 161, 39-49.

[7] C. Fan, D.L. Piron, P. Paradis, Electrochim. Acta 1994, 39, 2715-2722.

[8] B.E. Conway, L. Bai, J. Chem. Soc. Farady Trans. 1985, I(81), 1841-1862.

[9] I.A. Raj, V.K. Venkatesan, Int. J. Hydrogen Energy 1988, 13, 215-223.

[10] C. Fan, D.L. Piron, A. Sleb, P. Paradis, J. Electrochem. Soc. 1994, 141, 382-391.

[11] J. Divisek, H. Schmitz, J. Balej, J. Appl. Electrochem. 1989, 19, 519-530.

[12] A. Lasia, A. Rami, J. Electroanal. Chem. 1990, 294, 123-141.

[13] J.M. Jakšić, M.V. Vojnović, N.V. Krstajić, Electrochim. Acta 2000, 45, 4151-4158.

[14] M.R. Gennero de Chialvo, A.C. Chialvo, J. Electroanal. Chem. 1998, 448, 87-93.

[15] M.M. Jakšić, Mat. Chem. Phys. 1989, 22, 1-26.

[16] Y. Liang, S. Yang, Z. Yi, X. Lei, J. Sun, Y. Zhou, Mat. Sci. Eng. B 2005, 121, 152-155.

[17] G. Kreysa, B. Hokansson, P. Egdunge, Electrochim. Acta 1988, 33, 1351-1357.

[18] N. Krstajić, M. Popović, B. Grgur, M. Vojnović, D. Šepa, J. Electroanal. Chem. 2001, 512, 16-26.

[19] Handbook of Chemistry and Physics, 57th ed., CRC Press Inc, Cleveland, 1976-1977, p. B133.

[20] U. Lačnjevac, B.M. Jović, Z. Baščarević, V.M. Maksimović, V.D. Jović, Electrochim. Acta 2009, 54, 3115-3123.

[21] V.D. Jović, B.M. Jović, U. Lačnjevac, G. Branković, S. Bernik, A. Rečnik, Electrochim. Acta 2010, 55, 4188-4193.

[22] C.A. Marozzi, A.C. Chialvo, Electrochim. Acta 2000, 45, 2111-2120.

[23] C.A. Marozzi, A.C. Chialvo, Electrochim. Acta 2001, 46, 861-866.

IZVOD

Skoro sve komercijalne katode u industrijskim procesima izdvajanja vodonika, naročito one koje se primenjuju u procesu hlor-alkalne elektrolize, baziraju se na prevlakama koje sadrže plemenite metale (Pt,Ru,Ir itd.). U ovom radu je izvršen pokušaj da se, na osnovu teorije elektrokatalize izdvajanja vodonika, elektrohemijski istalože kompozitne katodne prevlake na bazi Ni sa uključkom MoO$_3$ ili MoO$_2$ čestica i da se ispita njihovo ponašanje u uslovima industrijskog izdvajanja vodonika. Pokazano je da je moguće dobiti prevlake koje imaju iste karakteristike kao komercijalne katode. Da bi se definisali optimalni uslovi elektrohemijskog taloženja ovih prevlaka ispitivane su njihove osobine (prenapetost za izdvajanje vodonika, sastav, fazni sastav i hrapavost površine) metodama skenirajuće elektronske mikroskopije i rendgenske analize.